

## Chemical microanalysis of mineral deposits on explanted hydrophilic acrylic intraocular lenses

S.E. AVETISOV, A.A. GAMIDOV, I.A. NOVIKOV, A.A. FEDOROV, A.A. KAS'YANOV

Research Institute of Eye Diseases, 11 A, B, Rossolimo St., Moscow, Russian Federation, 119021

**Aim** — to perform chemical microanalysis of mineral deposits on the surface of explanted hydrophilic acrylic intraocular lenses (IOL). **Material and methods.** Two soft IOLs made of hydrophilic acryl (one, however, hydrophobic surface coated) and explanted 3 and 6 years after implantation were examined by scanning electron microscopy (EVO LS10, Carl Zeiss, Germany). Chemical composition of the lens surface was studied using an energy-dispersive spectrometer (EDS X-Max50, Oxford, Great Britain). **Results.** Chemical microanalysis allowed identification of the deposits, which turned out to be non-stoichiometric hydroxylapatite (also, hydroxyapatite (HA)) crystals with zinc impurity (up to 1.4%weight). **Conclusion.** The two samples represent two stages of a single process. The early stage is associated with newly formed crystals that are unable to cause any significant changes to the lens surface. However, as spherocrystals grow, they exert a crystallization effort that moves their growth centers apart with subsequent lens rupture and deformation. Crystal morphology undergoes dynamic changes: while primary (newly formed) crystals are sheaf-like, mature are spheres. A growing HA is non-stoichiometric. Zinc abundance accounts for appearance of its separate mineral phase. Hydrophilic properties of acrylic polymer determine high affinity for HA crystals. Hydrophobic coating (sample no.1) does not completely prevent lens opacification due to mineral deposits on its surface.

**Keywords:** opacification, IOL, acrylic, hydrophilic, hydrophobic coating, hydroxylapatite, crystals.

*Vestnik\_Oftalmology\_2015-4\_74EN*

The great variety of modern intraocular lenses (IOLs) facilitates optimal choice in each patient. Desirable characteristics are the following: wide optical power range, ease of implantation, ultraviolet (UV) protection of the retina, resistance to laser treatment, and biocompatibility with eye tissues. These requirements are pretty much met by the most popular type of IOLs - soft acrylic (either hydrophobic, or hydrophilic). Hydrophilic acrylic lenses are currently gaining an even wider clinical usage due to mature production technology and less significant photopsias as compared to hydrophobic analogues. According to the literature, however, hydrophilic acrylic IOLs as well as those made of polymethyl methacrylate (PMMA) or silicone are liable to irreversible opacification, especially in the presence of ocular and/or systemic comorbidity [1-6]. In a number of cases they even have to be explanted due to loss of transparency [7]. Hence, in medically compromised patients, hydrophobic IOLs with lower opacification rates might be a better option.

Studies on the mechanisms of IOL opacification published to date are rather descriptive and contain mostly slit lamp biomicroscopy and optical microscopy data. Chemical microanalysis of surface deposits on explanted IOLs has been attempted by only a few foreign authors [3,4,8]. Supposedly, the gap is due to limited availability of specialized and expensive equipment.

The aim of this study was to perform chemical microanalysis of mineral deposits on the surface of explanted hydrophilic acrylic IOLs.

### Material and methods

Two opacified soft IOLs made of hydrophilic acryl explanted 3 and 6 years after implantation were selected: 1 – an Oculentis LS-312-1Y hydrophobic surface coated lens, Germany; 2 – a PhysIOL Micro+A 123 lens, Belgium. In both cases the patient's visual acuity was significantly reduced due to loss of IOL transparency. All examinations were held in the Laboratory of Fundamental Research in Ophthalmology at the Research Institute of Eye Diseases, Moscow. Low vacuum (70 Pa) scanning electron microscopy of the lenses was performed on EVO LS10 machine (Carl Zeiss, Germany). Microtopography of the samples was determined with secondary electrons (SE) at accelerating voltage of 10-20 kV and probe current of 0.6-1 nA.

Chemical composition of the lens surface was studied using a backscattered electron detector (NT-BSD) and Oxford X-Max50 energy-dispersive spectrometer (United Kingdom). Original AzTec software (Oxford, United Kingdom).

#### For correspondence:

Gamidov Alibek Abdulmutalimovich, MD, PhD, senior research associate in the Laboratory of New Laser Technologies  
e-mail: algam@bk.ru

dom) was used for analyses enabling micromapping of element distributions.

## Results and discussion

Surface topography of the two lenses obtained by SEM agreed with their appearance under optical microscope.

Thus, light optical microscopy of Sample 1 revealed a diffuse white film on both anterior and posterior IOL surfaces. In SE-images, it consisted of isometric tubercle-like precipitates sized 3-5  $\mu\text{m}$  and tending to merge. The density of this fine-grained film was uneven. Most of the precipitates were uniformly distributed across the surface of the optic at a density of 60-70 elements per 100  $\mu\text{m}^2$ , but accumulated (up to 80-100 elements per 100  $\mu\text{m}^2$ ) at technological irregularities, for example, a crater-like impression in the periphery (Fig. 1). Changes of the haptics were similar but less significant.

SE-images of Sample 2 showed that the center of its anterior surface was occupied by compact groups of large (10-20  $\mu\text{m}$ ) polygonal concentric granules separated by multidirectional wedge-shaped grooves (ruptures in the lens surface) (Fig. 2). The density of the opacification was generally even - about 30-40 granules per 100  $\mu\text{m}^2$ . As just mentioned, all the granules were concentric. Each had a prominent nucleation zone surrounded by rhythmic growth zones of unequal brightness that reflect changes in crystal chemistry during its ontogenesis. Along the boundaries of the solid opacification, IOL surface was deformed and elevated like a crater rim, while the central region of the area involved was slightly depressed.

In both cases, BSE-images revealed an excess of elements with large atomic masses (lately identified as P, Ca, and Zn) in the area of opacification as compared to the average composition of uninvolved lens surface. The results of spectral microanalysis of the deposits are plotted as graphs in Figure 3. In a BSE-image of Sample 1 (Fig. 4), one can see numerous reflective inclusions within individual deposits in the form of sheaf-like split crystals. Sample 2 is notable fully-formed spherocrystals with radial concentric zoning (Fig. 5).

Energy-dispersive spectrometry revealed that chemical composition of the deposits on either lens is identical and that they are, in fact, hydroxylapatite (also, hydroxyapatite, or HA) crystals with zinc impurity (up to 1.4wt%).

Taking into account that Ca ions in a hydroxylapatite are unlikely to be replaced by Zn, one can assume that two

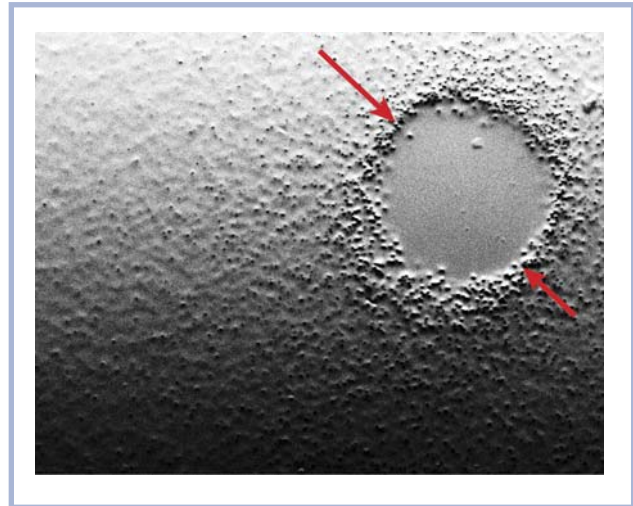


Fig. 1. IOL microtopography, sample 1.

The whole lens is covered by a diffuse fine-grained film, more dense at surface irregularities such as the crater-like impression shown here (arrows).



Fig. 2. IOL microtopography, sample 2.

Numerous concentric deposits compactly located in the centre of the anterior surface of the lens optic.

separate mineral phases are involved here: hydroxylapatite itself, which is predominant, and some other phosphate like, for example, kleemanite, whose ideal formula is  $\text{ZnAl}_2(\text{PO}_4)_2(\text{OH})_2 \cdot 3\text{H}_2\text{O}$ . In our samples, the assumed kleemanite accounted for no more than 9mol%. Hydroxylapatite and Zn-bearing phase formulas and content are given in the Table.

### Chemical composition of surface deposits on the two IOLs

Sample	Hydroxylapatite formula $\text{Ca}_3(\text{PO}_4)_3(\text{OH})$ (normalized by phosphorus)	Content in the mineral phase, %	Assumed kleemanite formula $\text{ZnAl}_2(\text{PO}_4)_2(\text{OH})_2 \cdot 3\text{H}_2\text{O}$ (normalized by zinc)	Content in the mineral phase, %
1	$(\text{Ca}_{4.7}, \text{Mg}_{0.2}, \text{Na}_{0.1})(\text{PO}_4)_3(\text{OH})$	95	$\text{Zn}(\text{Al}_{1.6}, \text{Si}_{0.3})(\text{PO}_4)_{1.8}(\text{OH})_2 \cdot 3\text{H}_2\text{O}$	5
	$(\text{Ca}_{4.6}, \text{Mg}_{0.4})(\text{PO}_4)_3(\text{OH})$	97	$\text{Zn}(\text{Al}_{1.9}, \text{Si}_{0.2})(\text{PO}_4)_{1.8}(\text{OH})_2 \cdot 3\text{H}_2\text{O}$	3
	$(\text{Ca}_{4.6}, \text{Mg}_{0.3}, \text{Na}_{0.1})(\text{PO}_4)_3(\text{OH})$	100	—	—
2	$(\text{Ca}_{4.8}, \text{Na}_{0.3})(\text{PO}_4)_3(\text{OH})$	91	$\text{Zn}(\text{Al}_{1.8}, \text{Si}_{0.1})(\text{PO}_4)_{1.8}(\text{OH})_2 \cdot 3\text{H}_2\text{O}$	9
	$(\text{Ca}_{4.7}, \text{Na}_{0.1})(\text{PO}_4)_3(\text{OH})$	93	$\text{Zn}(\text{Al}_{1.9})(\text{PO}_4)_2(\text{OH})_{1.8} \cdot 3\text{H}_2\text{O}$	7
	$(\text{Ca}_{4.7}, \text{Na}_{0.3})(\text{PO}_4)_3(\text{OH})$	93	$\text{Zn}(\text{Al}_{1.7}, \text{Si}_{0.1})(\text{PO}_4)_{1.7}(\text{OH})_2 \cdot 3\text{H}_2\text{O}$	7

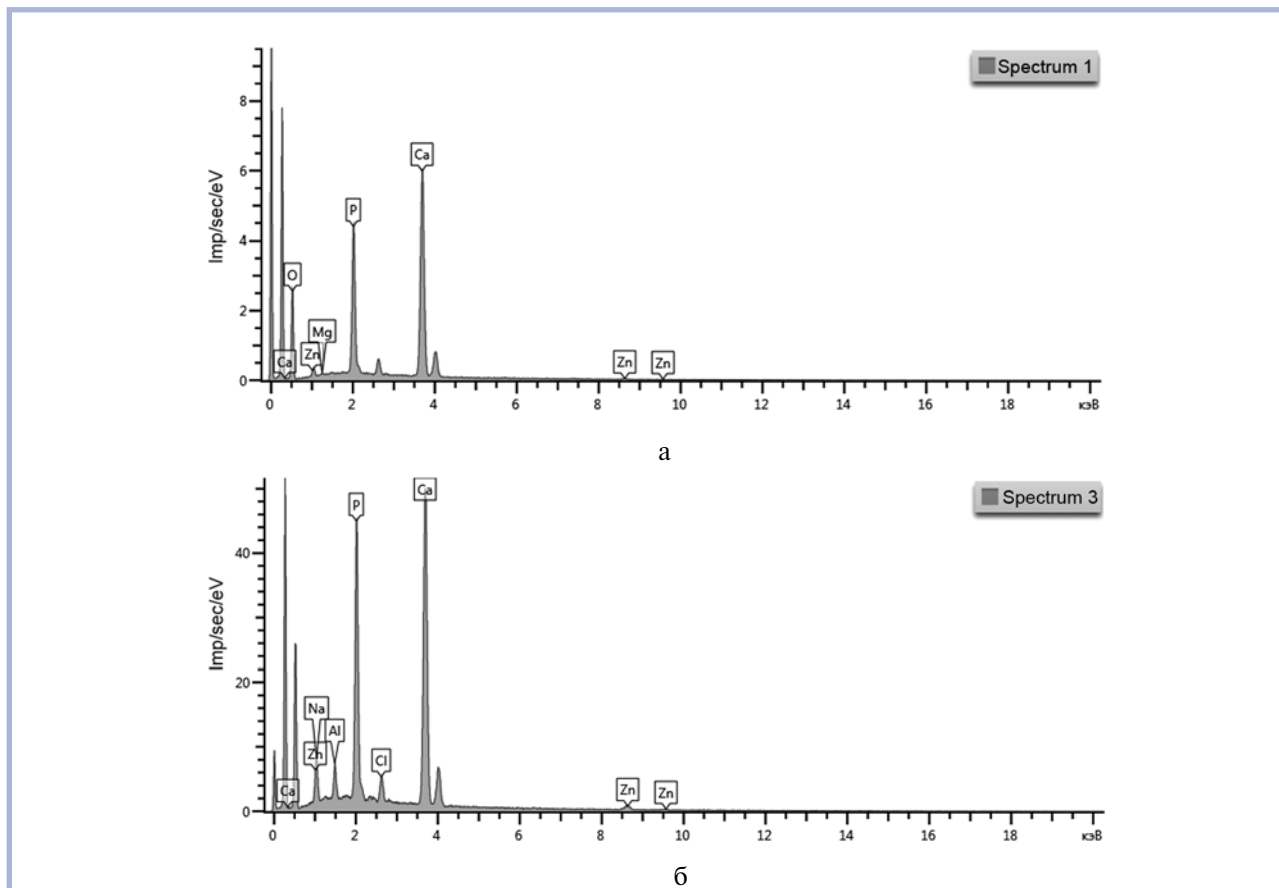


**Fig. 3. Graphical presentation of spectral results for surface deposits on lens samples 1 and 2.**  
 The deposits are composed predominantly of elements with high atomic masses (P, Ca, Zn).

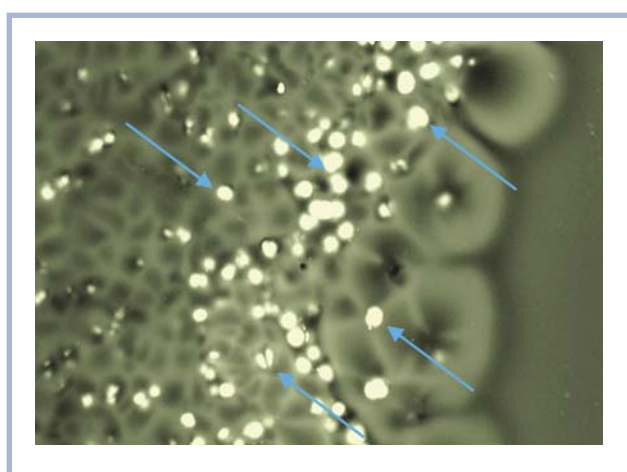


**Fig. 4. Scanning electron microscopy of sample 1. Multiple reflective inclusions within individual deposits in the form of sheaf-like split crystals (arrows).**

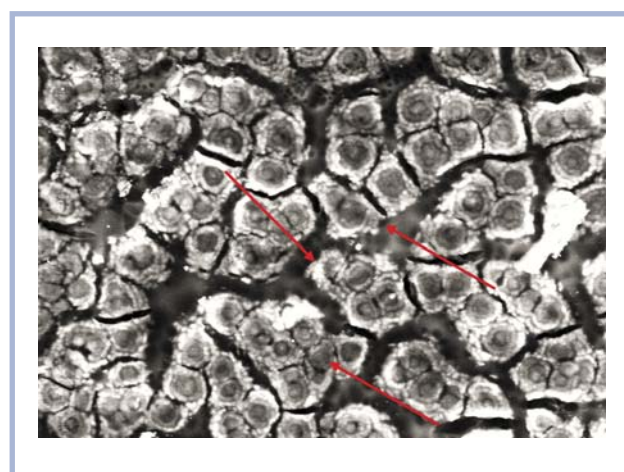


**Fig. 5. Scanning electron microscopy of sample 2. Fully-formed spherocrystals with radial concentric zoning (arrows).**

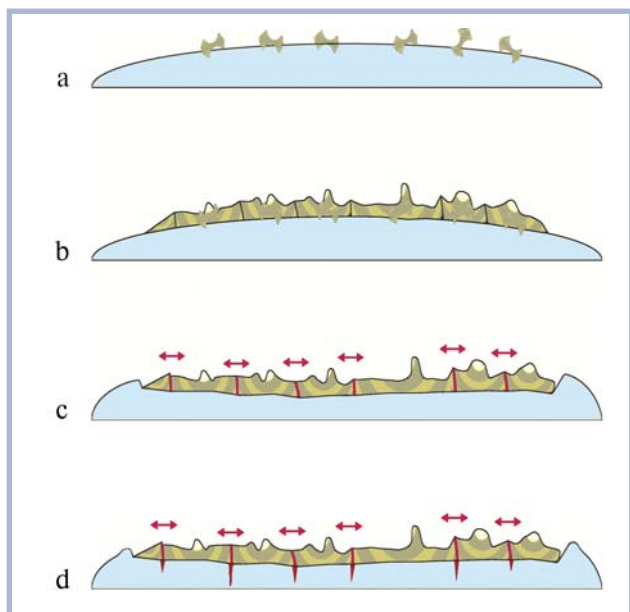


**Fig. 6. A schematic interpretation of the possible pathological process on the IOL surface.**

a — crystal nucleation; b — merging of growing spherocrystals; c — distancing of crystal growth centers; d — lens surface rupture and deformation.

## Conclusion

Hydroxylapatite affinity to IOL surface is determined by hydrophilic properties of acrylic polymer itself. However, hydrophobic surface coated lenses are still not proof of mineral deposits.

## REFERENCES

- Gamidov A.A., Kasjanov A.A., Fedorov A.A., Siplivy V.I. Clinical cases of transparency disturbance of acrylic IOL. *Prakticheskaja Medicina*. 2012; 59(4): 267–270. Available at: <http://pmarchive.ru/klinicheskie-sluchai-narusheniya-prozrachnosti-akrilovyx-iol/>. Accessed January 05, 2015. (In Russ.)
- Chuikova S.A., Verzin A.A., Malyugin B.E., Shkvorchenko D.O. Klinicheskie sluchai pomutneniya gidrofil'nykh intraokulyarnykh linz v pozd-nem posleoperatsionnom periode [Clinical cases of opacity of hydrophilic intraocular lenses in the late postoperative period]. Available at: <http://www.eyepress.ru/article.aspx?9302>. Accessed January 05, 2015. (In Russ.)
- Kleinmann G., Apple D.J., Werner L., Pandey S.K., Neuhann I.M., Assia E.I., Laws D.E., de Borin O.A., Mamalis N. Postoperative surface deposits on intraocular lenses in children. *Journal of Cataract & Refractive Surgery*. 2006; 32(11): 1932–1937. doi.org/10.1016/j.jcrs.2006.06.035
- Neuhann I.M., Werner L., Izak A.M., Pandey S.K., Kleinmann G., Mamalis N., Neuhann T., Apple D. Late postoperative opacification of a Hydrophilic acrylic (Hydrogel) intraocular lens. A clinicopathological analysis of 106 explants. *Ophthalmology*. 2004; 111(11):2094–2101. doi:10.1016/j.ophtha.2004.06.032
- Oner H.F., Durak I., Saatci O.A. Late postoperative opacification of a Hydrophilic acrylic intraocular lens. *J. Ophthalmic Surgery, Lasers & Imaging*. 2002; 33(4): 304–308. doi: 10.3928/1542-8877-20020701-09
- Werner L. Causes of intraocular lens opacification or discoloration. *Journal of Cataract & Refractive Surgery*. 2007;33(4):713–726. doi:10.1016/j.jcrs.2007.01.015
- Mamalis N., Brubaker J., Davis D., Espandar L., Werner L. Complications of foldable intraocular lenses requiring explantation or secondary intervention — 2007 survey update. *Journal of Cataract & Refractive Surgery*. 2008; 34(9): 1584–1591. doi:10.1016/j.jcrs.2008.05.046
- Neuhan I.M., Kleinmann G., Apple D.J. A new classification of calcification of intraocular lenses. *Ophthalmology*. 2008; 115(1): 73–79. doi.org/10.1016/j.ophtha.2007.02.016

Received 07.07.14

The two cases presented here are likely to be part of the same process that takes place on the IOL surface. Severe imperfections in the growing HA crystals lead to dynamic changes of their morphology. As soon as new crystals are nucleated they split forming numerous sheaf-like structures that later grow into complete spherocrystals. Note that spherocrystals, while small, are unable to cause any significant harm to the lens (Fig. 6, a), but as they grow and merge (Fig. 6, b), they exert a crystallization effort that moves their growth centers apart (Fig. 6, c) with subsequent lens surface rupture and deformation (Fig. 6, d).

Trying to normalize atomic ratios of mineral deposits on the IOL surfaces by the ideal hydroxylapatite formula we faced a mismatch. In particular, we found decreased mineral stoichiometry and significant zinc impurity (up to 1.4wt%), which suggests that ‘our’ aggregates are poly-mineral.

The discovery of high Zn concentrations may become a turning point in the study of surface precipitation mechanisms in IOLs. Sources of zinc and its role in metabolic pathways as well as the conditions under which Zn-bearing deposits can be formed are yet to be revealed.

### Author contributions:

Study conception and design — S.A., A.G.  
Acquisition and handling of data — A.G., I.N., A.K.  
Statistical analysis of data — I.N., A.G.  
Drafting of manuscript — A.G., I.N.  
Critical revision — S.A.

**The authors declare no conflict of interest.**